2. Steady-State Neutronics Methodology

2.1 Cartesian Geometry

2.1.1 Nodal Expansion Method

The nodal expansion method (NEM) [1,2,3] starts with the multigroup neutron diffusion equation in P_1-form.

$$\nabla \cdot J_g(r) + [\Sigma_{ag}(r) + \sum_{g'>g} \Sigma_{gg'}(r)]\varphi_g(r) = \sum_{g'<g} \Sigma_{g'g}(r)\varphi_{g'}(r) + \frac{1}{k}\sum_{g'} \sum_{j} \chi_{pg}^{j} \nu\Sigma_{fg'}^{j}(r)\varphi_{g'}(r) + \chi_{ex} S_g^{ext}(r) \quad (2.1\text{-}1a)$$

$$J_g(r) + D_g(r)\nabla\varphi_g(r) = 0 \quad (2.1\text{-}1b)$$

where φ_g = neutron flux in group g,

J_g = neutron current in group g,

Σ_{ag} = absorption cross section in group g,

$\Sigma_{g'g}$ = scattering cross section from g′ to g,

$\nu\Sigma_{fg}^{j}$ = ν-fission cross section of fissionable isotope j in group g,

k = eigenvalue,

χ_{pg}^{j} = prompt fission spectrum of fissionable isotope j in group g,

χ_{ex} = external source spectrum in group g,

S_g^{ext} = external source in group g.

Integrating Eq. (2.1-1) over a node volume leads to the exact nodal balance equation as follows:

$$\sum_{u=x,y,z} \frac{1}{a_u^m}\left[\left(j_{gul}^{-m} + j_{gur}^{+m}\right) - \left(j_{gul}^{+m} + j_{gur}^{-m}\right)\right] + \left(\Sigma_{ag}^m + \sum_{g'>g} \Sigma_{gg'}^m\right)\phi_g^m$$
$$= \sum_{g'<g} \Sigma_{g'g}^m \phi_{g'}^m + \frac{1}{k}\sum_{g'}\sum_{j} \chi_{pg}^j \nu\Sigma_{fg'}^{jm}\phi_{g'}^m \qquad (2.1\text{-}2a)$$

$$j_{gus}^{+m} - j_{gus}^{-m} = -D_g^m \left.\frac{\partial \psi_{gu}^m}{\partial u}\right|_s \qquad (2.1\text{-}2b)$$

where a_u^m = mesh size in the direction u (=x,y,z) of node m,

$j_{gus}^{\pm m}$ = incoming and outgoing currents in group g at the surfaces s (=l,r) of node m.

The notations are clarified in Fig. 2-1. The surface average fluxes are defined by

$$\psi_{gus}^m = \frac{1}{A_u^m}\int_0^{a_v^m}\int_0^{a_w^m} \varphi_g(r)\,dv\,dw \qquad (2.1\text{-}3)$$

where A_u^m = transverse area to u-direction.

The surface average fluxes can be expanded into a quartic polynomial

$$\psi_g^m(u) = \sum_{i=0}^{4} a_{igu}\,\xi_i(u) \qquad (2.1\text{-}4)$$

where $\xi_0(u) = 1$,

$\xi_1(u) = 2u - 1$,

$\xi_2(u) = 6u(1-u) - 1$,

$\xi_3(u) = 6u(1-u)(2u-1)$,

$\xi_4(u) = 6u(1-u)(5u^2 - 5u + 1)$.

The first three coefficients of the right hand side of Eq. (2.1-4) can be expressed by nodal balance equations and continuity conditions, and the third and fourth order coefficients a_{3gu} and a_{4gu} can be determined by solving the 1-dimensional equivalent diffusion equations:

$$-\frac{\partial}{\partial u}D_g^m\frac{\partial}{\partial u}\psi_{gu}^m+(\Sigma_{agu}^m+\sum_{g'>g}\Sigma_{gg'u}^m)\psi_{gu}^m = \sum_{g'<g}\Sigma_{g'gu}^m\psi_{g'u}^m+\frac{1}{k}\sum_{g'}\sum_j\chi_{pg}^j\nu\Sigma_{fg'}^{jm}\psi_{g'u}^m-D_g^mL_{gu}^m \tag{2.1-5}$$

where $L_{gu}^m=-\frac{1}{A_u^m}\int_0^{a_v^m}\int_0^{a_w^m}(\frac{d^2}{dv^2}+\frac{d^2}{dw^2})\varphi_g(r)dvdw$

To find a_{0gu} one can integrate the transverse integrated flux over the u-direction and to obtain a_{1gu} and a_{2gu} one can evaluate the transverse integrated flux at the surfaces of the node in the u-direction. The complete polynomial form of Eq. (2.1-4) can be then written as follows:

$$\psi_{gu}(u)=\phi_g\xi_0(u)+\frac{\psi_{gur}-\psi_{gul}}{2}\xi_1(u)+(\phi_g-\frac{\psi_{gur}+\psi_{gul}}{2})\xi_2(u) + a_{3gu}\xi_3(u)+a_{4gu}\xi_4(u). \tag{2.1-6}$$

Using the diffusion theory expression $\psi_{gus}^m=2(j_{gus}^{+m}+j_{gus}^{-m})$ and inserting Eq. (2.1-6) into Eq. (2.1-2b), the equations for the outgoing currents on the left and right surfaces are given as functions of the incoming currents and the nodal flux.

$$\begin{aligned} j_{gul}^{-m}&=c_{1gu}^m(\phi_g^m+a_{4gu})+c_{2gu}^mj_{gul}^{+m}+c_{3gu}^mj_{gur}^{-m}-c_{4gu}^ma_{3gu}\\ j_{gur}^{+m}&=c_{1gu}^m(\phi_g^m+a_{4gu})+c_{3gu}^mj_{gul}^{+m}+c_{2gu}^mj_{gur}^{-m}+c_{4gu}^ma_{3gu}\end{aligned} \tag{2.1-7}$$

The coefficients of the outgoing currents equations are rational functions of $D_{gu}=D_g^m/a_u$,

where D_g^m is the diffusion constant of energy group g.

$$c_{1gu} = \frac{D_{gu}}{1/6 + 2D_{gu}}, \qquad c_{2gu} = 1 - 4c_{1gu} - c_{3gu}, \tag{2.1-8}$$

$$c_{3gu} = \frac{-c_{1gu}}{3/4 + 3D_{gu}}, \qquad c_{4gu} = c_{1gu} - 6D_{gu}c_{3gu}.$$

The final form of the nodal balance equations Eq. (2.1-2a) becomes

$$\begin{aligned}(\Sigma_{ag}^m + \sum_{g'>g}\Sigma_{gg'}^m + \sum_{u=x,y,z}\frac{2c_{1gu}^m}{a_u^m})\phi_g^m \\ = \sum_{g'<g}\Sigma_{g'g}\phi_{g'}^m + \frac{1}{k}\sum_{g'}\sum_{j}\chi_{pg}^j \nu\Sigma_{fg'}^{jm}\phi_{g'}^m \\ + \sum_{u=x,y,z}\frac{1}{a_u^m}\left[(1 - c_{2gu}^m - c_{3gu}^m)(j_{gul}^{+m} + j_{gur}^{-m}) - 2c_{1gu}^m a_{4gu}^m\right]\end{aligned} \tag{2.1-9}$$

and this can be solved iteratively.

According to the weighted residual method, integrating Eq. (2.1-5) with the weighting function ξ_1 or ξ_2 presented in Eq. (2.1-4) results in the following form:

$$\begin{aligned}(60\frac{D_{gu}}{a_u} + \Sigma_g)a_{3gu} = -\frac{5}{3}\Sigma_g a_{1gu} \\ + \sum_{g'<g}\Sigma_{g'g}(\frac{5}{3}a_{1g'u} + a_{3g'u}) \\ + \sum_{g'}(\frac{5}{3}a_{1g'u} + a_{3g'u})\frac{1}{k}\sum_{j}\chi_{pg}^j \nu\Sigma_{fg'}^j \\ - \frac{5}{3}D_g b_{1gu}\end{aligned} \tag{2.1-10a}$$

$$
\begin{aligned}
(140\frac{D_{gu}}{a_u}+\Sigma_g)a_{4gu} &= \frac{7}{3}\Sigma_g a_{2gu} \\
&+\sum_{g'<g}\Sigma_{g'g}(-\frac{7}{3}a_{2g'u}+a_{4g'u}) \\
&+\sum_{g'}(-\frac{7}{3}a_{2g'u}+a_{4g'u})\frac{1}{k}\sum_j \chi_{pg}^j \nu\Sigma_{fg'}^j \\
&+\frac{7}{3}D_g b_{2gu}
\end{aligned}
\qquad \text{(2.1-10b)}
$$

where $\Sigma_g = \Sigma_{ag} + \sum_{g'>g}\Sigma_{gg'}$,

b_{1gu} , b_{2gu} = coefficients of the transverse leakage expansion function (see Eq.(5-1)).

One can obtain the coefficients a_{3gu} and a_{4gu} with Eqs. (2.1-10a) and (2.1-10b). For the acceleration of an iterative solution, a vectorized red-black Gauss-Seidel method, a multi-level coarse-mesh rebalancing and an asymptotic extrapolation are used. These will be discussed for details later in this manual.

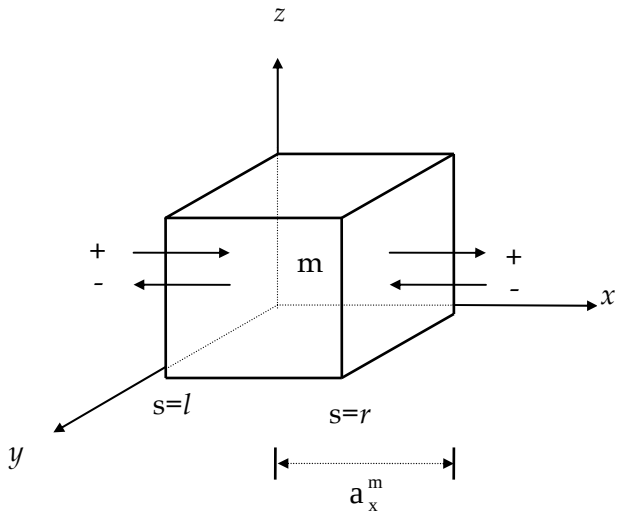

Figure 2-1 Illustration of Mesh Geometry

2.1.2 Nodal Integration Method

The Nodal Integration Method (NIM) [4] is shortly characterized by exact integration of resulting 1-dimensional equation with the transverse leakage shape approximated by a parabola. The starting point for the derivation of NIM is a set of equivalent 1-D diffusion equations.

$$\begin{aligned} D_1 \frac{d^2\psi_{1u}}{du^2} - \Sigma_{r1}\psi_{1u} + \frac{\nu\Sigma_{f2}}{k}\psi_{2u} &= D_1 L_{1u} \\ D_2 \frac{d^2\psi_{2u}}{du^2} - \Sigma_{a2}\psi_{2u} + \Sigma_{12}\psi_{1u} &= D_2 L_{2u} \end{aligned} \tag{2.1-11}$$

where D_g = diffusion coefficient of group g,

L_{gu} = transverse leakage of group g in u-direction,

$\Sigma_{r1} = \Sigma_{a1} + \Sigma_{12} - \frac{\nu\Sigma_{f1}}{k}$.

The transverse leakage L_{gu} is orthogonal to the spatial direction u. The equations above can be rewritten as

$$\begin{aligned} \frac{d^2\psi_{1u}}{du^2} - c_1\psi_{1u} + c_2\psi_{2u} &= L_{1u} \\ \frac{d^2\psi_{2u}}{du^2} - c_3\psi_{2u} + c_4\psi_{1u} &= L_{2u} \quad (u = x, y, z) \end{aligned} \tag{2.1-12}$$

where $c_1 = \frac{\Sigma_{r1}}{D_1}, c_2 = \frac{\nu\Sigma_{f2}}{D_1 k}, c_3 = \frac{\Sigma_{a2}}{D_2}, c_4 = \frac{\Sigma_{12}}{D_2}$.

This is a coupled system of ordinary, linear, inhomogeneous differential equations of second order with constant coefficients. The equations above can be solved analytically with a quadratic approximation of the one-dimensional transverse leakages

$$L_{gu} = \sum_{v=0}^{2} b_{gv} \xi_v(u) \tag{2.1-13}$$

where $\xi_0(u) = 1$,

$\xi_1(u) = 2u - 1$,

$\xi_2(u) = 6u(1-u) - 1$.

The solution can be expressed as

$$\psi_{1u} = k_1 \cosh\kappa_1 u + k_2 \sinh\kappa_1 u + \alpha(k_3 \cos\kappa_2 u + k_4 \sin\kappa_2 u) + \sum_{v=0}^{2} f_{1v} \xi_v(u) \tag{2.1-14}$$

$$\psi_{2u} = \beta(k_1 \cosh\kappa_1 u + k_2 \sinh\kappa_1 u) + k_3 \cos\kappa_2 u + k_4 \sin\kappa_2 u + \sum_{v=0}^{2} f_{2v} \xi_v(u)$$

The eigenvalues are derived from

$$\kappa_{1,2}^2 = \frac{c_1 + c_3}{2} \pm \sqrt{(\frac{c_1 - c_3}{2})^2 + c_2 c_4} \tag{2.1-15}$$

The coupling parameters are

$$\alpha = \frac{c_2}{c_1 - \kappa_2^2}, \beta = \frac{c_4}{c_3 - \kappa_1^2}. \tag{2.1-16}$$

The solution is simplified in reflector nodes since α vanishes. The eigenvalues are as follows:

$$\kappa_1^2 = c_1, \kappa_2^2 = c_3, c_1 \neq c_3.$$

The flux continuity condition is used to determine the coefficients f_{gv} of the inhomogeneous

part of the solution. The node average flux ϕ_g results from the integration of the 1-D flux solution over the total node length in u-direction.

$$\phi_g = \frac{1}{a}\int_0^a \psi_{gu}\,du \tag{2.1-17}$$

where a = node width.

The integration of Eq. (2.1-17) leads to the following matrix:

$$\begin{bmatrix} f_{10} \\ f_{20} \end{bmatrix} = \begin{bmatrix} \phi_1 \\ \phi_2 \end{bmatrix} - \begin{bmatrix} \frac{\sinh\kappa_1 a}{\kappa_1 a} & \frac{\cosh\kappa_1 a - 1}{\kappa_1 a} & \alpha\frac{\sin\kappa_2 a}{\kappa_2 a} & \alpha\frac{1-\cos\kappa_2 a}{\kappa_2 a} \\ \beta\frac{\sinh\kappa_1 a}{\kappa_1 a} & \beta\frac{\cosh\kappa_1 a - 1}{\kappa_1 a} & \frac{\sin\kappa_2 a}{\kappa_2 a} & \frac{1-\cos\kappa_2 a}{\kappa_2 a} \end{bmatrix} \begin{bmatrix} k_1 \\ k_2 \\ k_3 \\ k_4 \end{bmatrix} \tag{2.1-18}$$

The coefficients f_{g1} and f_{g2} are obtained by inserting Eq. (2.1-14) into Eq. (2.1-12) and by comparing the coefficients of the linearly independent expansion functions ξ_1 and ξ_2, respectively.

$$\begin{bmatrix} f_{1i} \\ f_{2i} \end{bmatrix} = \frac{1}{c_2 c_4 - c_1 c_3} \begin{bmatrix} c_3 & c_2 \\ c_4 & c_1 \end{bmatrix} \begin{bmatrix} b_{1i} \\ b_{2i} \end{bmatrix}, \quad (i = 1, 2). \tag{2.1-19}$$

The node boundary conditions are used to determine the integration constants k_i (i=1,..,4) and written as

$$\begin{aligned} 4j^+_{gul} &= \psi_g(0) - 2D_g \left.\frac{d\psi_{gu}}{du}\right|_{u=0} \\ 4j^-_{gur} &= \psi_g(a) + 2D_g \left.\frac{d\psi_{gu}}{du}\right|_{u=a} \end{aligned} \tag{2.1-20}$$

where j^{+}_{gul} = incoming current on the left boundary of a node,

j^{-}_{gur} = incoming current on the right boundary of a node.

The incoming currents of the node concerned are obtained using the continuity conditions. To simplify notation the incoming current vector $\mathbf{J}^{in}_{u}$ is written as

$$\mathbf{J}^{in}_{u} = \left[j^{+}_{1ul},\ j^{+}_{2ul},\ j^{-}_{1ur},\ j^{-}_{2ur} \right]^{T} \tag{2.1-21}$$

where the superscript T denotes transposition.

In the same manner the following vectors are introduced.

$$\tilde{\mathbf{\Phi}} = \left[\phi_1,\ \phi_2,\ \phi_1,\ \phi_2 \right]^{T} \tag{2.1-22}$$

$$\mathbf{V} = 4\left[-\frac{D_1}{a}(f_{11} + 3f_{12}),\ -\frac{D_2}{a}(f_{21} + 3f_{22}),\ \frac{D_1}{a}(f_{11} - 3f_{12}),\ \frac{D_2}{a}(f_{21} - 3f_{22}) \right]^{T}$$

$$\mathbf{W} = \left[-f_{11} - f_{12},\ -f_{21} - f_{22},\ f_{11} - f_{12},\ f_{21} - f_{22} \right]^{T}$$

The evaluation of the node boundary conditions then results in

$$4\mathbf{J}^{in}_{u} = \mathbf{Q}\left[k_1, k_2, k_3, k_4 \right]^{T} + \mathbf{V} + \mathbf{W} + \tilde{\mathbf{\Phi}} \tag{2.1-23}$$

where $\mathbf{Q}$ is a 4x4 matrix. The constants k_i are formally determined by the incoming currents, the node average fluxes and the transverse leakages. For the construction of an efficient iteration algorithm the diffusion boundary condition

$$\psi_u = 2(\mathbf{J}^{in}_{u} + \mathbf{J}^{out}_{u}) \tag{2.1-24}$$

yields

$$\mathbf{J}_u^{out} = \frac{1}{2}\mathbf{P}\left[k_1, k_2, k_3, k_4\right]^T + \frac{1}{2}(\mathbf{W} + \mathbf{\Phi} - \mathbf{J}_u^{in} \tag{2.1-25}$$

where $\mathbf{P}$ is a 4x4 matrix. By eliminating the integration constants the outgoing currents in direction u can be obtained. Denoting the fourth order unity matrix as $\mathbf{I}_4$ leads to the resulting outgoing current equation

$$\mathbf{J}_u^{out} = \frac{1}{2}(\mathbf{P}_u\mathbf{Q}_u^{-1} - \mathbf{I}_4)(4\mathbf{J}_u^{in} - \mathbf{V}_u - \mathbf{W}_u - \mathbf{\Phi} + \mathbf{J}_u^{in} - \frac{1}{2}\mathbf{V}_u . \tag{2.1-26}$$

The multiplication of matrices $\mathbf{PQ}^{-1}$ can favorably be partitioned into 2x2 submatrices $\mathbf{E}$ and $\mathbf{F}$, respectively to reveal its high degree of symmetry.

$$\mathbf{PQ}^{-1} = \begin{bmatrix} \mathbf{E} & \mathbf{F} \\ \mathbf{F} & \mathbf{E} \end{bmatrix} \tag{2.1-27}$$

The node average fluxes are solutions of the nodal balance equation in which the nodal leakage is represented by the difference between incoming and outgoing currents. If the outgoing currents are eliminated from the nodal balance equation, the node average fluxes can be calculated as functions of the incoming currents and the transverse leakages.

The corresponding nodal balance equation is written in matrix notation

$$\begin{bmatrix} \Sigma_{r1} & -\frac{\nu\Sigma_{f2}}{k} \\ -\Sigma_{21} & \Sigma_{a2} \end{bmatrix} \begin{bmatrix} \phi_1 \\ \phi_2 \end{bmatrix} = \begin{bmatrix} \mathbf{I}_2 & \mathbf{I}_2 \end{bmatrix} \sum_{u=x,y,z} \frac{1}{a_u}(\mathbf{J}_u^{in} - \mathbf{J}_u^{out}) \tag{2.1-28}$$

After the outgoing currents $\mathbf{J}_u^{out}$ are eliminated in this equation and some mathematical manipulations are performed, the nodal balance equation for the determination of the node average flux can be obtained :

$$\begin{bmatrix} \Sigma_{r1} - H_{11} & -\dfrac{\nu\Sigma_{f2}}{k} - H_{12} \\ -\Sigma_{21} - H_{21} & \Sigma_{a2} - H_{22} \end{bmatrix} \begin{bmatrix} \phi_1 \\ \phi_2 \end{bmatrix} = \begin{bmatrix} \mathbf{I}_2 & \mathbf{I}_2 \end{bmatrix} \sum_{u=x,y,z} \frac{1}{2a_u} \left[(\mathbf{P}_u \mathbf{Q}_u^{-1} - \mathbf{I}_4)(\mathbf{V}_u + \mathbf{W}_u - 4\mathbf{J}_u^{in}) + \mathbf{V}_u \right] \tag{2.1-29}$$

where $H_{11} = \sum_{u=x,y,z} \frac{1}{a_u}(E_{u11} + F_{u11} - 1)$, $H_{12} = \sum_{u=x,y,z} \frac{1}{a_u}(E_{u12} + F_{u12})$,

$H_{21} = \sum_{u=x,y,z} \frac{1}{a_u}(E_{u21} + F_{u21})$, $H_{22} = \sum_{u=x,y,z} \frac{1}{a_u}(E_{u22} + F_{u22} - 1)$.

2.1.3 AFEN/NEM Hybrid Method

Analytic Function Expansion Nodal Method (AFEN) [5,6] directly solves the multi-dimensional diffusion equation instead of the transverse-averaged one-dimensional one. It is based on analytic basis functions satisfying the diffusion equation at any points of the node. The flux expansion consisting of basis functions includes non-separable cross terms which are coupled to other spatial directions. AFEN determines all nodal unknowns such as node average, surface average and corner-point fluxes by means of the nodal coupling equations which comprise the nodal balance equation for node average flux, the interface current continuity condition for surface fluxes and Corner-Point Balance Method (CPB) [7] or Method of Successive Smoothing (MSS) [8] for corner fluxes. In the AFEN/NEM hybrid method [9], NEM is used for the axial direction where the neutronic coupling is relatively weak compared to the radial direction. For the application of coarse-mesh rebalancing (CMR) acceleration scheme [9] , a response matrix formulation of the AFEN/NEM hybrid method is derived.

In order to solve the two-group two-dimensional diffusion equation, λ_g^n is defined as the eigenvalue of matrix $(\mathbf{D}^n)^{-1}[\mathbf{\Sigma}^n - (1/k_{eff})\ \boldsymbol{\nu}\mathbf{\Sigma}_f^n]$ and $\mathbf{R}^n$ as the 2x2 matrix with columns of the corresponding eigenvectors. In addition, ξ is introduced as:

$$\xi^n(x,y) = (\mathbf{R}^n)^{-1}\,\boldsymbol{\Phi}^n(x,y) \tag{2.1-30}$$

which satisfies the partial differential equation:

$$\nabla^2\xi_g^n(x,y) - \lambda_g^n\xi_g^n(x,y) = 0 \tag{2.1-31}$$

The general solution of the above equation can be expressed in the following form:

$$\xi_g^n(x,y) = \sum_{i=0}^{\infty}\{A_{gi}^n SN\kappa_g^n(\alpha_{gxi}^n x + \alpha_{gyi}^n y) + B_{gi}^n CS\kappa_g^n(\alpha_{gxi}^n x + \alpha_{gyi}^n y)\} \tag{2.1-32}$$

where $\kappa_g^n = \sqrt{|\lambda_g^n|}$,

$$(\alpha_{gxi}^n)^2 + (\alpha_{gyi}^n)^2 = 1,$$

$$SN\kappa_g^n(\alpha_{gxi}^n x + \alpha_{gyi}^n y) = \begin{cases}\sinh\kappa_g^n(\alpha_{gxi}^n x + \alpha_{gyi}^n y) & \lambda_g^n > 0\\ \sin\kappa_g^n(\alpha_{gxi}^n x + \alpha_{gyi}^n y) & \lambda_g^n < 0\end{cases},$$

$$CS\kappa_g^n(\alpha_{gxi}^n x + \alpha_{gyi}^n y) = \begin{cases}\cosh\kappa_g^n(\alpha_{gxi}^n x + \alpha_{gyi}^n y) & \lambda_g^n > 0\\ \cos\kappa_g^n(\alpha_{gxi}^n x + \alpha_{gyi}^n y) & \lambda_g^n < 0\end{cases}.$$

The sets of $(\alpha_{gxi}^n, \alpha_{gyi}^n)$ are chosen as (1, 0), (0, 1), ($\sqrt{2}/2$, $\sqrt{2}/2$) and (-$\sqrt{2}/2$, $\sqrt{2}/2$), which are distributed 45 degrees apart on a unit circle. Thus, the intranodal flux expansion consists of a set of eight basis functions:

$$\begin{aligned}\xi(x,y) = {} & C_g^n + A_{g1}^n SN\kappa_g^n x + A_{g2}^n CS\kappa_g^n x + A_{g3}^n SN\kappa_g^n y + A_{g4}^n CS\kappa_g^n y\\ & + B_{g1}^n SN\frac{\sqrt{2}}{2}\kappa_g^n x SN\frac{\sqrt{2}}{2}\kappa_g^n y + B_{g2}^n SN\frac{\sqrt{2}}{2}\kappa_g^n x CS\frac{\sqrt{2}}{2}\kappa_g^n y\\ & + B_{g3}^n CS\frac{\sqrt{2}}{2}\kappa_g^n x SN\frac{\sqrt{2}}{2}\kappa_g^n y + B_{g4}^n CS\frac{\sqrt{2}}{2}\kappa_g^n x CS\frac{\sqrt{2}}{2}\kappa_g^n y\end{aligned} \tag{2.1-33}$$

In the response matrix formulation of this method, however, interface partial currents are used as the nodal unknowns instead of corresponding surface fluxes. Once all the

coefficients in the flux expansion are expressed in terms of the nodal unknowns for the response matrix formulation, we build as many solvable nodal coupling equations as the number of these unknowns to be determined.

The first set of nodal coupling equations to be solved for the node-average flux can be obtained by integrating Eq. (2.1-2a) over a node volume:

$$\Sigma_{rg}\phi_g + \sum_{d=x,y,z}\frac{1}{a_d}\left[\left(j^{out}_{gdr} - j^{in}_{gdr}\right) + \left(j^{out}_{gdl} - j^{in}_{gdl}\right)\right] = \sum_{g'<g}\Sigma_{g'g}\phi_{g'} + \frac{1}{k_{eff}}\sum_{g'}\chi_g \nu\Sigma_{fg'}\phi_{g'} \tag{2.1-34}$$

The second set of nodal coupling equations for the surface average partial currents are derived by applying continuity condition of the net neutron currents across the node interface and the diffusion approximation relating partial currents with net currents and surface fluxes. The node outgoing partial current can then be expressed in terms of incoming partial currents, node average fluxes and corner fluxes. For example, the interface partial currents in x-direction on the right-hand side as illustrated in Fig. 2-2 is

$$\mathbf{J}^{out}_r = \frac{\mathbf{P}_1 + \mathbf{P}_2}{2}\mathbf{J}^{in}_r + \frac{\mathbf{P}_1 - \mathbf{P}_2}{2}\mathbf{J}^{in}_l + \frac{1}{4}(\mathbf{1} - \mathbf{P}_1)\,\overline{\boldsymbol{\Phi}} + \frac{\mathbf{P}_3 + \mathbf{P}_4}{2}\delta\boldsymbol{\Phi}_r + \frac{\mathbf{P}_3 - \mathbf{P}_4}{2}\delta\boldsymbol{\Phi}_l \tag{2.1-35}$$

where $\mathbf{J}^{out}_s$ = outgoing partial current at surface s,

$\mathbf{J}^{in}_s$ = incoming partial current at surface s,

$\overline{\boldsymbol{\Phi}}$ = node average flux,

$\delta\boldsymbol{\Phi}_s$ = difference between averaged corner flux and corner flux determined at each adjacent node (s = l, r),

$\mathbf{P}_i$ = coupling coefficient,

$\mathbf{1}$ = unity matrix,

subscript r, l = right and left surfaces.

In the above equation, the coupling coefficients $\mathbf{P}_i$'s are constant matrices whose elements depend on k_{eff} and the group constants of the node. The MSS or CPB can be used to solve the corner fluxes, which form the third set of nodal coupling equations. This will be described in details in Section 8.

The axial intranodal distribution in this method is determined by solving the transverse-integrated one-dimensional equivalent diffusion equation in the axial direction by the nodal expansion method (NEM), since the spatial coupling in the axial direction is relatively weak when compared to that for the radial direction.

$$
\begin{aligned}
&-\frac{\partial}{\partial z} D_g^m \frac{\partial}{\partial z} \psi_g^m(z) + (\Sigma_{ag}^m + \sum_{g'>g} \Sigma_{gg'}^m) \psi_g^m(z) \\
&\quad = \sum_{g'<g} \Sigma_{g'g}^m \psi_{g'}^m(z) + \frac{1}{k} \sum_{g'} \sum_{j} \chi_{pg}^j \nu \Sigma_{fg'}^{jm} \psi_{g'}^m(z) - D_g^m L_g^m(z)
\end{aligned}
\qquad (2.1\text{-}36)
$$

The term $-D_g L_g(z)$ in Eq. (2.1-36) is the transverse leakage. The surface average flux $\psi_g(z)$ can be expanded into a quartic polynomial with orthogonal functions (see Eq. (2.1-4)). The outgoing partial currents on the left and right surfaces of a node in the axial direction are given by Eq. (2.1-7).

2.1.4 Non-linear Nodal Expansion Method

In the non-linear nodal expansion method (NNEM) [10], both the coarse-mesh finite difference (CMFD) method and the two-node NEM method are used for the solution of the multi-group diffusion equation. The node current of the CMFD method is given as follows:

$$J_{gu}^{m\pm} = \mp \tilde{D}_{gu}^{m\pm} \left(\phi_g^{m\pm1} - \phi_g^{m} \right) \tag{2.1-37}$$

where $\tilde{D}_{gu}^{m\pm} = \dfrac{2\, D_g^{m\pm1}\, D_g^{m}}{D_g^{m\pm1}\, a_{u,m} + D_g^{m}\, a_{u,m\pm1}}$.

The assumption of linear flux variation is not accurate for the large node size. Thus this method involves iterations between solutions of the CMFD problem and the two-node NEM problems. The CMFD problem incorporates the global coupling of the nodes while the two-node problems incorporates local higher order coupling. The method is nonlinear because the coefficient matrix for the CMFD problem contains the nodal coupling coefficients which need to be updated by the two-node calculations during the iteration.

In the two-node NEM calculation, the interface current is obtained by solving the NEM equations for the two-node problem in which the flux solution of the previous CMFD problem is used as the boundary condition. The two-node problem calculation is performed for every interface of all nodes and all directions to provide an improved estimate of the net current. The interface current is then used to determine a corrective nodal coupling coefficient, $\hat{D}_{gu}^{m+}$, such that the following expression can be reproduced for the NEM based interface current.

$$J_{gu}^{m\pm} = \mp \tilde{D}_{gu}^{m\pm} \left(\phi_g^{m\pm1} - \phi_g^{m} \right) \mp \hat{D}_{gu}^{m+} \left(\phi_g^{m\pm1} + \phi_g^{m} \right) \tag{2.1-38}$$

The next CMFD problem is formulated using the above relation for the current. The second term of RHS of Eq. (2.1-38) can be regarded as a correction term which corrects the error of the linear flux used to obtain the first term.

The two-node problem produces 8 unknowns per energy group which can be solved with 8 conditions: two nodal balance equations, one current continuity condition, one flux continuity condition and four moment equations. The definition and derivation of NEM are the same as in Section 2.1.1.

2.1.5 Non-linear Analytic Nodal Method

The non-linear nodal analytic method (NANM) [11] is basically the same as the NNEM described in the preceding section except for the main kernel to update the interface current. For correction of the interface current, it uses the analytic nodal method (ANM) instead of NEM.

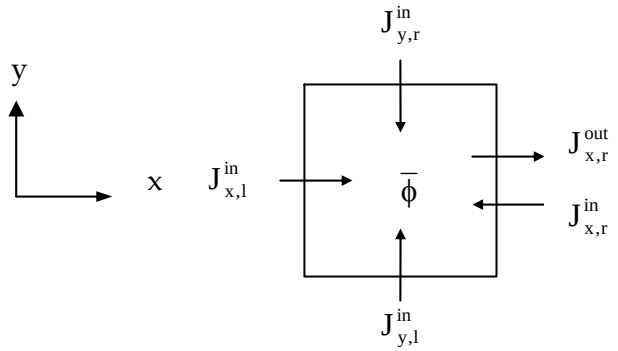

Figure 2-2 Indices of Partial Currents and Node Average Flux in a Rectangular Node

2.2 Hexagonal Geometry

2.2.1 AFEN/NEM Hybrid Method

The AFEN method [12] directly solves the multi-dimensional diffusion equation instead of the transverse-integrated one-dimensional diffusion equations by expanding the solution into non-separable analytic basis functions, which satisfy the diffusion equation at any points of the node. The flux expansion consisting of basis functions includes non-separable cross terms which are coupled to other spatial directions. The AFEN method determines all nodal unknowns such as node average, surface average and corner-point flux by means of the nodal coupling equations which comprise the nodal balance equation and the interface current continuity condition. In the AFEN/NEM hybrid method [13], NEM is used for the axial direction where the neutronic coupling is relatively weak compared to the radial direction. For the application of coarse-mesh rebalancing (CMR) acceleration scheme, a response matrix formulation of the AFEN/NEM hybrid method is derived.

AFEN for two-dimensional geometry is based on decoupling the multigroup diffusion equations for a node n into the "mode-group" partial differential equations

$$\nabla^2 \xi_g^n(x,y) - \lambda_g^n \xi_g^n(x,y) = 0 \qquad (2.2\text{-}1)$$

by defining $\xi^n(x,y) = (\mathbf{R}^n)^{-1}\phi^n(x,y)$. Here, λ_g^n 's are the eigenvalues of matrix $(\mathbf{D}^n)^{-1}[\mathbf{\Sigma}^n - (1/k_{eff})\ \boldsymbol{\nu}\mathbf{\Sigma}_f^n]$ and $\mathbf{R}^n$ is the matrix with columns of the corresponding eigenvectors. The general solution of the Eq. (2.2-1) can be expressed as:

$$\xi_g^n(x,y) = \sum_{i=0}^{\infty}\{A_{gi}^n SN\kappa_g^n(\alpha_{gxi}^n x + \alpha_{gyi}^n y) + B_{gi}^n CS\kappa_g^n(\alpha_{gxi}^n x + \alpha_{gyi}^n y)\} \qquad (2.2\text{-}2)$$

where $\kappa_g^n = \sqrt{|\lambda_g^n|}$,

$(\alpha_{gxi}^n)^2 + (\alpha_{gyi}^n)^2 = 1$,

$$SN\kappa_g^n(\alpha_{gxi}^n x+\alpha_{gyi}^n y)=\begin{cases}\sinh \kappa_g^n(\alpha_{gxi}^n x+\alpha_{gyi}^n y) & \lambda_g^n>0\\ \sin \kappa_g^n(\alpha_{gxi}^n x+\alpha_{gyi}^n y) & \lambda_g^n<0\end{cases},$$

$$CS\kappa_g^n(\alpha_{gxi}^n x+\alpha_{gyi}^n y)=\begin{cases}\cosh \kappa_g^n(\alpha_{gxi}^n x+\alpha_{gyi}^n y) & \lambda_g^n>0\\ \cos \kappa_g^n(\alpha_{gxi}^n x+\alpha_{gyi}^n y) & \lambda_g^n<0\end{cases}.$$

In the regular hexagonal node the AFEN method adopts one node-average flux, six interface fluxes, and six corner fluxes per group as the nodal unknowns and expands the intranodal flux distribution in the node into twelve analytic basis functions and one additional constant term. The sets of $(\alpha_{gxi}^n, \alpha_{gyi}^n)$ in Eq. (2.2-1) are chosen with the same constraints applied to the rectangular geometry. They are (1, 0), (0, 1), ($\sqrt{3}$/2, 1/2), (-$\sqrt{3}$/2, 1/2), (1/2, $\sqrt{3}$/2) and (1/2, -$\sqrt{3}$/2), which are the coordinates evenly distributed 30 degrees apart on a unit circle. Introducing three Cartesian coordinate systems, (x,y), (u,v) and (p,q) for the convenience of handling the hexagonal node, the intranodal flux distribution of the node is expressed as:

$$\begin{aligned}\xi_g^n(x,y) = C_g &+ A_{g1}^x SN\kappa_g^n x + B_{g1}^x CS\kappa_g^n x + A_{g2}^x SN\kappa_g^n y + B_{g2}^x CS\kappa_g^n y\\ &+ A_{g1}^p SN\kappa_g^n p + B_{g1}^p CS\kappa_g^n p + A_{g2}^p SN\kappa_g^n q + B_{g2}^p CS\kappa_g^n q\\ &+ A_{g1}^u SN\kappa_g^n u + B_{g1}^u CS\kappa_g^n u + A_{g2}^u SN\kappa_g^n v + B_{g2}^u CS\kappa_g^n v\end{aligned} \qquad (2.2\text{-}3)$$

where $u=-\frac{1}{2}x-\frac{\sqrt{3}}{2}y$, $v=\frac{\sqrt{3}}{2}x-\frac{1}{2}y$, $p=-\frac{1}{2}x+\frac{\sqrt{3}}{2}y$, $q=-\frac{\sqrt{3}}{2}x-\frac{1}{2}y$.

In the response matrix formulation of this method [13], however, interface partial currents are used as the nodal unknowns instead of corresponding surface fluxes. Once all the coefficients in the flux expansion Eq. (2.2-3) are expressed in terms of the nodal unknowns for the response matrix formulation, we build as many solvable nodal coupling equations as the number of these unknowns to be determined. The first set of nodal coupling equations to be solved for the node-average flux can be obtained by integrating Eq. (2.1-2a) over a node volume. The second set of nodal coupling equations for the surface average partial currents are derived by applying continuity condition of the net neutron

currents across the node interface and the diffusion approximation relating partial currents with net currents and surface fluxes. The node outgoing partial current can then be expressed in terms of incoming partial currents, node average fluxes and corner fluxes. For example, the interface partial currents in x-direction on the right-hand side as illustrated in Fig. 2-3 is

$$\begin{aligned}\mathbf{J}^{out}_{x,r} = &\frac{\mathbf{P}_1+\mathbf{P}_2}{2}\mathbf{J}^{in}_{x,r} + \frac{\mathbf{P}_1-\mathbf{P}_2}{2}\mathbf{J}^{in}_{x,l} \\ &+ (\mathbf{P}_3+\mathbf{P}_4)\frac{\mathbf{J}^{in}_{u,l}+\mathbf{J}^{in}_{p,l}}{2} + (\mathbf{P}_3-\mathbf{P}_4)\frac{\mathbf{J}^{in}_{u,r}+\mathbf{J}^{in}_{p,r}}{2} \\ &+ (\mathbf{P}_5+\mathbf{P}_6)\frac{\boldsymbol{\Phi}_{u,r}+\boldsymbol{\Phi}_{p,l}}{2} + (\mathbf{P}_5-\mathbf{P}_6)\frac{\boldsymbol{\Phi}_{u,l}+\boldsymbol{\Phi}_{p,r}}{2} \\ &+ \mathbf{P}_7\frac{\boldsymbol{\Phi}_{x,l}+\boldsymbol{\Phi}_{x,r}}{2} + \frac{1}{4}(\mathbf{I}+\mathbf{P}_1+2\mathbf{P}_3+8\mathbf{P}_5+4\mathbf{P}_7)\,\overline{\boldsymbol{\Phi}}\end{aligned} \tag{2.2-4}$$

where $\mathbf{J}^{out}_{d,s}$ = outgoing partial current vector in d- direction at surface s,

$\mathbf{J}^{in}_{d,s}$ = incoming partial current vector in d- direction at surface s,

$\boldsymbol{\Phi}_{d,s}$ = corner flux vector in d-direction at surface s,

$\overline{\boldsymbol{\Phi}}$ = node average flux vector,

$\mathbf{P}_i$ = coupling coefficient matrix.

In the above equation, the coupling coefficients are constant matrices whose elements depend on k_{eff} and the group constants of the node. By applying the corner point balance (CPB) scheme for the corner flux evaluation in hexagonal node, the set of nodal coupling equations for the corner-point fluxes can be derived in terms of surface average fluxes and node average fluxes. It forms the third set of nodal coupling equations and it will be described in details in Section 8.2.2.

The axial intranodal distribution is determined by solving the transverse-integrated one-dimensional equivalent diffusion equation in the axial direction by the nodal expansion method (NEM). The definition and derivation of NEM are the same as in Section 2.1.3.

2.2.2 Non-linear Local Fine-mesh Method

The objective of the two-node problem to be solved for the application of the nonlinear iteration technique is to find the surface-averaged current at the interface of the two nodes, given the group constants, k_{eff}, current profiles at the transverse surfaces, and node average fluxes. To accomplish the objective, the intra-nodal flux distribution satisfying the constraint on the node average fluxes should be determined first. The intranodal flux distribution within the two hexagons can be represented in terms of mesh-averaged fluxes if the finite difference scheme is used. [14]

Suppose that a hexagon is divided into N thin trapezoids as shown in Fig. 2-4. The mesh spacing is rather desirable, in the aspect of computational efficiency, to have tightly spaced meshes only near the interface of the two hexagons since the current at the interface is the one to be evaluated with sufficient accuracy. For the i-th trapezoid, a mesh-averaged flux (ϕ_i) and surface-averaged normal neutron currents (J_i^R, J_i^L , J_i^T , J_i^B) can be defined. Then the neutron balance equation in a energy group is given as:

$$J_i^R h_{i+1} - J_i^L h_i + \Sigma \phi_i V_i = -(J_i^T - J_i^B)\, l_i \tag{2.2-5}$$

where J_i^S (with the superscript S being L, R, B, and T) and ϕ_i are two element vectors, h_i, l_i, and V_i are the height at the left side, the length of the top (and bottom) side and the volume of mesh i, respectively, and Σ is a 2x2 matrix consisting of two group constants as:

$$\Sigma \equiv \begin{bmatrix} \Sigma_{r1} - \lambda\nu\Sigma_{f1} & -\lambda\nu\Sigma_{f2} \\ -\Sigma_{12} & \Sigma_{r2} \end{bmatrix}, \ \lambda = \frac{1}{k_{eff}} \tag{2.2-6}$$

By using the finite difference approximation, the currents at the left and right boundaries of a node can be obtained in a conventional way. The neutron balance equation given by Eq. (2.2-7) holds for all the interior meshes except the two meshes located at the left and the right boundaries of the two-node problem in which no boundary condition is given. Thus there are only 2*(N-1) balance equations available per group for the 2N unknowns. The additional two equations needed for a unique solution come from the constraints on the

node average flux.

$$\frac{1}{V_H}\sum_{i=1}^{N}\phi_i V_i = \bar{\phi}_L\,, \qquad \frac{1}{V_H}\sum_{i=N+1}^{2N}\phi_i V_i = \bar{\phi}_R \tag{2.2-9}$$

where V_H is the volume of the hexagon.

The linear system consisting of Eq. (2.2-5) for meshes 2 through 2N-1 and Eq. (2.2-9) is primarily a block tridiagonal system with nonzero off-diagonal elements mostly at the last two rows. The left-hand side of the linear system is shown schematically below:

$$A\phi = \begin{bmatrix} d_2 & \alpha_3 & & & & & & \alpha_2 \\ \alpha_3 & \ddots & \ddots & & & & & \\ & \ddots & d_n & \alpha_{n+1} & & & & \\ & & \alpha_{n+1} & d_{n+1} & \ddots & & & \\ & & & \ddots & \ddots & \alpha_{2n-1} & & \\ & & & & \alpha_{2n-1} & d_{2n-1} & \alpha_{2n} & \\ & & & \beta_{n+1} & \cdots & \beta_{2n-1} & \beta_{2n} & \\ \beta_2 & \cdots & \beta_n & & & & & \beta_1 \end{bmatrix} \begin{bmatrix} \phi_2 \\ \vdots \\ \phi_n \\ \phi_{n+1} \\ \vdots \\ \phi_{2n-1} \\ \phi_{2n} \\ \phi_1 \end{bmatrix}. \tag{2.2-10}$$

Note that the basic element in the coefficient matrix is a 2x2 matrix.

It can be solved easily by using the Gauss Elimination technique because of the nearly tridiagonal structure. The fill-in problem will occur only at the last column and the last row during the Gauss Elimination and thus no significant computational burden will be encountered.

To obtain the currents at the external boundaries in which an albedo type of boundary condition is given, a set of one-node problems needs to be solved instead of the two-node problems. Similarly to the two-node problem, the one-dimensional one-node problem can be solved by the fine-mesh finite difference method (FDM).

The accuracy of a transverse-integrated method is limited by the accuracy of the profile of transverse current approximated by a low order function as long as the one-dimensional

problem is solved with sufficient accuracy. In order to obtain better profiles of transverse currents, two methods were applied. The first one is a simple vector addition scheme and is applied to the interior nodal interface. The other one is a more sophisticated method which utilizes a precalculated two-dimensional fine mesh solution for a hexagon located at the boundary when determining the current profile at an external surface as a superposition of the currents induced from the current sources placed at the other five surfaces. This method is used for the boundary surfaces in which the transverse leakage shape varies more drastically.

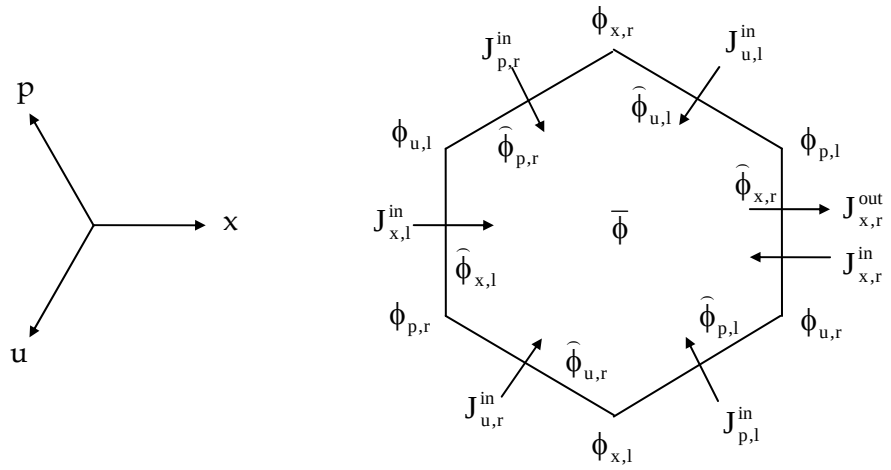

Figure 2-3 Indices of Currents and Fluxes in Hexagonal Geometry

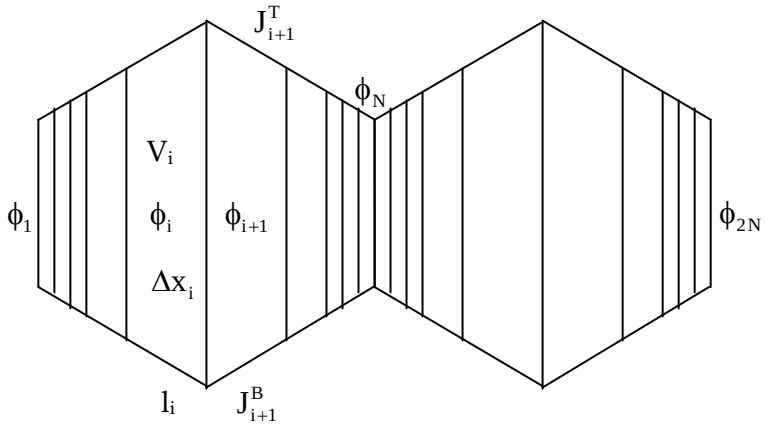

Figure 2-4 Fine Mesh Structure of a Two Hexagonal Node Problem

2.2.3 Non-linear Triangle-based Polynomial Expansion Nodal Method

In contrast with the non-linear local fine-mesh method that is based on two-node problem, the non-linear triangle-based polynomial expansion nodal (NTPEN) method [15,16] is based on one-node problem to find the outgoing partial currents and node average flux, given the group constants, k_{eff}, incoming partial currents, corner point fluxes. Instead of surface-based sweep of two-node problem, one-node problem sweeps the problem domain from node-base.

The non-linear triangle-based polynomial expansion nodal (NTPEN) method is a variation of the higher order polynomial expansion nodal (HOPEN) method [17] that solves the multi-group neutron diffusion equation in the hexagonal-z geometry. In contrast with the HOPEN method that represents the intranodal solution in a three-dimensional domain with a truncated polynomial expansion, only two-dimensional intranodal expansion is considered in the TPEN method for a triangular domain. The axial dependence of the intranodal flux is incorporated separately and it is determined by the nodal expansion method (NEM). For the consistency of node geometry of the other methods which are based on hexagon, TPEN solver is coded to solve one hexagonal node which is composed of 6 triangular nodes directly by Gauss elimination scheme.

Fig. 2-5 displays a triangular node and the nodal unknowns defined in the TPEN method. The nine unknowns are the volume average flux, first-order x- and y-moments, three surface average fluxes and three corner fluxes, respectively. A truncated polynomial expansion of the intranodal flux in the two-dimensional domain that is consistent with the nine unknowns can be set as:

$$\phi_g^m(x,y) = c_{g0}^m + a_{gx}^m x + a_{gy}^m y + b_{gx}^m x^2 + b_{gu}^m u^2 + b_{gp}^m p^2 + c_{gx}^m x^3 + c_{gu}^m u^3 + c_{gp}^m p^3. \qquad (2.2\text{-}11)$$

Once the polynomial approximation of the intranodal flux distribution is made, the nine unknowns are uniquely determined from nine constraints, one nodal balance equation, two weighted residual equations, three surface current conditions and three corner point leakage conditions. For these equations, the following two-dimensional neutron diffusion equation

can be constructed:

$$-D_g^m\left(\frac{\partial^2}{\partial x^2}+\frac{\partial^2}{\partial y^2}\right)\phi_g^m(x,y)+\Sigma_{rg}^m\phi_g^m(x,y) = \frac{\chi_g}{k_{eff}}\sum_{g'}\nu\Sigma_{fg'}^m\phi_{g'}^m(x,y)+\sum_{g'}\Sigma_{sgg'}^m\phi_{g'}^m(x,y)+S_{gz}^m(x,y), \tag{2.2-12}$$

where $S_{gz}^m(x,y)$ is axial source distribution which comes from axial leakage.

The nine constraints to determine the nine nodal unknowns can be derived as the following form from the definitions of each constraint:

Nodal Balance Equation:

$$\left(80\frac{D_g^m}{h^2}+\Sigma_{rg}^m\right)\bar{\phi}_g^m = \frac{\chi_g}{k_{eff}}\sum_{g'}\nu\Sigma_{fg'}^m\bar{\phi}_{g'}^m+\sum_{g'}\Sigma_{sgg'}^m\bar{\phi}_{g'}^m+\bar{S}_{gz}^m + 32\frac{D_g^m}{h^2}\left(\bar{\phi}_{gx}^m+\bar{\phi}_{gu}^m+\bar{\phi}_{gp}^m\right)-\frac{16}{3}\frac{D_g^m}{h^2}\left(\phi_{gx}^m+\phi_{gu}^m+\phi_{gp}^m\right). \tag{2.2-13}$$

Weighted residual equation using $w(x,y)=x$:

$$\left(80\frac{D_g^m}{h^2}+\Sigma_{rg}^m\right)\tilde{\phi}_{gx}^m = \frac{\chi_g}{k_{eff}}\sum_{g'}\nu\Sigma_{fg'}^m\tilde{\phi}_{g'x}^m+\sum_{g'}\Sigma_{sgg'}^m\tilde{\phi}_{g'x}^m+\tilde{S}_{gzx}^m + \frac{8}{3}\frac{D_g^m}{h^2}\left(2\bar{\phi}_{gx}^m-\bar{\phi}_{gu}^m-\bar{\phi}_{gp}^m\right)-\frac{8}{9}\frac{D_g^m}{h^2}\left(2\phi_{gx}^m-\phi_{gu}^m-\phi_{gp}^m\right). \tag{2.2-14}$$

Weighted residual equation using $w(x,y)=y$:

$$\left(80\frac{D_g^m}{h^2}+\Sigma_{rg}^m\right)\tilde{\phi}_{gy}^m = \frac{\chi_g}{k_{eff}}\sum_{g'}\nu\Sigma_{fg'}^m\tilde{\phi}_{g'y}^m+\sum_{g'}\Sigma_{sgg'}^m\tilde{\phi}_{g'y}^m+\tilde{S}_{gzy}^m - 8\frac{D_g^m}{h^2}\left(\bar{\phi}_{gu}^m-\bar{\phi}_{gp}^m\right)+\frac{8}{3}\frac{D_g^m}{h^2}\left(\phi_{gu}^m-\phi_{gp}^m\right). \tag{2.2-15}$$

Net current condition at boundary surfaces:

$$\bar{J}_{gx}^{m} = \frac{\sqrt{3}}{3}\frac{D_g^m}{h}\left\{2\phi_{gx}^{m} + \phi_{gu}^{m} + \phi_{gp}^{m} - 24\bar{\phi}_{gx}^{m} + 20\bar{\phi}_{g}^{m} + 120\tilde{\phi}_{gx}^{m}\right\}. \tag{2.2-16}$$

Net leakage condition at corner points:

$$L_{gx}^{m} = 4\sqrt{3}\frac{D_g^m}{h}\left\{-\phi_{gc} + \bar{\phi}_{gx}^{m} - 15\tilde{\phi}_{gx}^{m}\right\} \quad . \tag{2.2-17}$$

Fig. 2-6 shows 6 triangular nodes in a hexagonal node. For this hexagonal node, 6 incoming partial currents and 6 corner point fluxes are specified as the boundary conditions. Applying the TPEN to the six triangles yields 31 unknowns, 6 triangle node average fluxes, 6 *x*-moments, 6 *y*-moments, 6 inner surface fluxes, 6 outgoing partial currents and 1 center point flux. And Eqs. (2.2-13) through (2.2-17) are used to determine these unknowns. The resulting linear system to determine these unknowns is expressed as:

$$\begin{bmatrix} \mathbf{C_0} & \mathbf{0} & \mathbf{0} & \mathbf{-32C_1I_0} & \mathbf{-64C_1} & \mathbf{16/3\,C_1} \\ \mathbf{0} & \mathbf{C_0} & \mathbf{0} & \mathbf{8/3\,C_1I_0} & \mathbf{-32/3\,C_1} & \mathbf{16/9\,C_1} \\ \mathbf{0} & \mathbf{0} & \mathbf{C_0} & \mathbf{-8C_1I_1} & \mathbf{0} & \mathbf{0} \\ \mathbf{20I_2} & \mathbf{-60I_2} & \mathbf{60I_3} & \mathbf{-48I} & \mathbf{0} & \mathbf{2I} \\ \mathbf{20I} & \mathbf{120I} & \mathbf{0} & \mathbf{0} & \mathbf{-48I-\gamma} & \mathbf{2I} \\ \mathbf{0} & \mathbf{-15I_4} & \mathbf{0} & \mathbf{0} & \mathbf{2I_4} & \mathbf{-6i} \end{bmatrix} \begin{bmatrix} \bar{\varphi} \\ \tilde{\varphi}_x \\ \tilde{\varphi}_y \\ \bar{\varphi}_s \\ \mathbf{j_o} \\ \varphi_p \end{bmatrix} = \begin{bmatrix} \bar{S}_a \\ \tilde{S}_x \\ \tilde{S}_y \\ \bar{S}_s \\ \mathbf{S_j} \\ \mathbf{S_p} \end{bmatrix} \tag{2.2-18}$$

where

$$\mathbf{C_0} = \text{diag.}\left[\mathbf{a_0}\ \mathbf{a_0}\ \mathbf{a_0}\ \mathbf{a_0}\ \mathbf{a_0}\ \mathbf{a_0}\right] + 80\mathbf{C_1},\ \mathbf{C_1} = \text{diag.}\left[\mathbf{a_1}\ \mathbf{a_1}\ \mathbf{a_1}\ \mathbf{a_1}\ \mathbf{a_1}\ \mathbf{a_1}\right],$$

$$\boldsymbol{\gamma} = \text{diag.}\left[\mathbf{a_2}\ \mathbf{a_2}\ \mathbf{a_2}\ \mathbf{a_2}\ \mathbf{a_2}\ \mathbf{a_2}\right],\ \mathbf{I} = \text{dia.}\left[\mathbf{i}\ \mathbf{i}\ \mathbf{i}\ \mathbf{i}\ \mathbf{i}\ \mathbf{i}\right],\ \mathbf{I_0} = \begin{bmatrix} \mathbf{i} & \mathbf{i} & & & & \\ & \mathbf{i} & \mathbf{i} & & & \\ & & \mathbf{i} & \mathbf{i} & & \\ & & & \mathbf{i} & \mathbf{i} & \\ & & & & \mathbf{i} & \mathbf{i} \\ \mathbf{i} & & & & & \mathbf{i} \end{bmatrix},$$

$$\mathbf{I_1} = \begin{bmatrix} \mathbf{i} & \mathbf{-i} & & & & \\ & \mathbf{i} & \mathbf{-i} & & & \\ & & \mathbf{i} & \mathbf{-i} & & \\ & & & \mathbf{i} & \mathbf{-i} & \\ & & & & \mathbf{i} & \mathbf{-i} \\ \mathbf{-i} & & & & & \mathbf{i} \end{bmatrix},,\ \mathbf{I_2} = \begin{bmatrix} \mathbf{i} & & & & & \mathbf{i} \\ \mathbf{i} & \mathbf{i} & & & & \\ & \mathbf{i} & \mathbf{i} & & & \\ & & \mathbf{i} & \mathbf{i} & & \\ & & & \mathbf{i} & \mathbf{i} & \\ & & & & \mathbf{i} & \mathbf{i} \end{bmatrix},\ \mathbf{I_3} = \begin{bmatrix} \mathbf{i} & & & & & \mathbf{-i} \\ \mathbf{-i} & \mathbf{i} & & & & \\ & \mathbf{-i} & \mathbf{i} & & & \\ & & \mathbf{-i} & \mathbf{i} & & \\ & & & \mathbf{-i} & \mathbf{i} & \\ & & & & \mathbf{-i} & \mathbf{i} \end{bmatrix},$$

$$\mathbf{I}_4 = \left[\mathbf{i}\ \mathbf{i}\ \mathbf{i}\ \mathbf{i}\ \mathbf{i}\ \mathbf{i}\right],\ \bar{\boldsymbol{\varphi}} = \mathrm{row}\left[\bar{\boldsymbol{\varphi}}^1 \quad \bar{\boldsymbol{\varphi}}^2 \quad \cdots \quad \bar{\boldsymbol{\varphi}}^6\right],\ \tilde{\boldsymbol{\varphi}}_x = \mathrm{row}\left[\tilde{\boldsymbol{\varphi}}_x^1 \quad \tilde{\boldsymbol{\varphi}}_x^2 \quad \cdots \quad \tilde{\boldsymbol{\varphi}}_x^6\right],$$

$$\tilde{\boldsymbol{\varphi}}_y = \mathrm{row}\left[\tilde{\boldsymbol{\varphi}}_y^1 \quad \tilde{\boldsymbol{\varphi}}_y^2 \quad \cdots \quad \tilde{\boldsymbol{\varphi}}_y^6\right],\ \bar{\boldsymbol{\varphi}}_s = \mathrm{row}\left[\bar{\boldsymbol{\varphi}}_s^1 \quad \bar{\boldsymbol{\varphi}}_s^2 \quad \cdots \quad \bar{\boldsymbol{\varphi}}_s^6\right],$$

$$\mathbf{j}_o = \mathrm{row}\left[\mathbf{j}_o^1 \quad \mathbf{j}_o^2 \quad \cdots \quad \mathbf{j}_o^6\right],\ \boldsymbol{\varphi}_p = \begin{bmatrix}\phi_1^p \\ \phi_2^p\end{bmatrix},$$

$$\mathbf{a_0} = \begin{bmatrix}\Sigma_{r1} - \dfrac{1}{k_{eff}}\nu\Sigma_{f1} & -\dfrac{1}{k_{eff}}\nu\Sigma_{f2} \\ -\Sigma_{s21} & \Sigma_{r2}\end{bmatrix},\ \mathbf{a_1} = \frac{1}{h^2}\begin{bmatrix}D_1 & 0 \\ 0 & D_2\end{bmatrix},\ \mathbf{a_2} = \frac{\sqrt{3}h}{D_1 D_2}\begin{bmatrix}D_1 & 0 \\ 0 & D_2\end{bmatrix},$$

$$\mathbf{i} = \begin{bmatrix}1 & 0 \\ 0 & 1\end{bmatrix},\ \bar{\boldsymbol{\varphi}}^m = \begin{bmatrix}\bar{\phi}_1^m \\ \bar{\phi}_2^m\end{bmatrix},\ \tilde{\boldsymbol{\varphi}}_x^m = \begin{bmatrix}\tilde{\phi}_{1x}^m \\ \tilde{\phi}_{2x}^m\end{bmatrix},\ \tilde{\boldsymbol{\varphi}}_y^m = \begin{bmatrix}\tilde{\phi}_{1y}^m \\ \tilde{\phi}_{2y}^m\end{bmatrix},\ \bar{\boldsymbol{\varphi}}_s^m = \begin{bmatrix}\bar{\phi}_{1s}^m \\ \bar{\phi}_{2s}^m\end{bmatrix},\ \mathbf{j}_o^m = \begin{bmatrix}\bar{J}_{1o}^m \\ \bar{J}_{2o}^m\end{bmatrix},$$

m=1,…,6.

The above linear system (2.2-18) can be solved directly by a block Gaussian Elimination scheme provided the aforementioned boundary conditions.

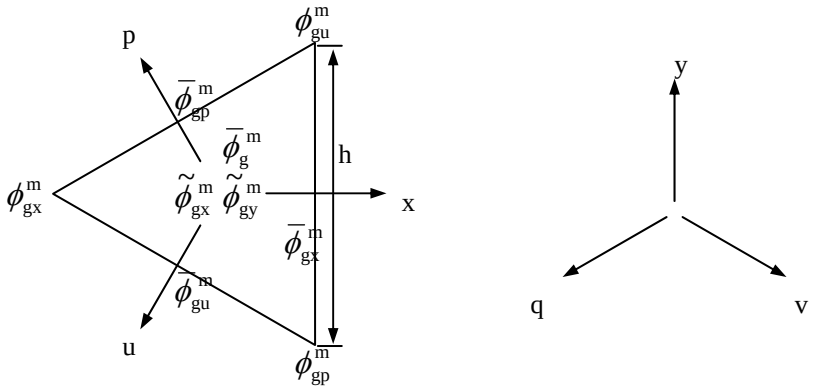

$$V^m = \text{node volume} = \frac{\sqrt{3}}{4} h^2$$

Figure 2-5. Unknowns and Coordinates for the TPEN method

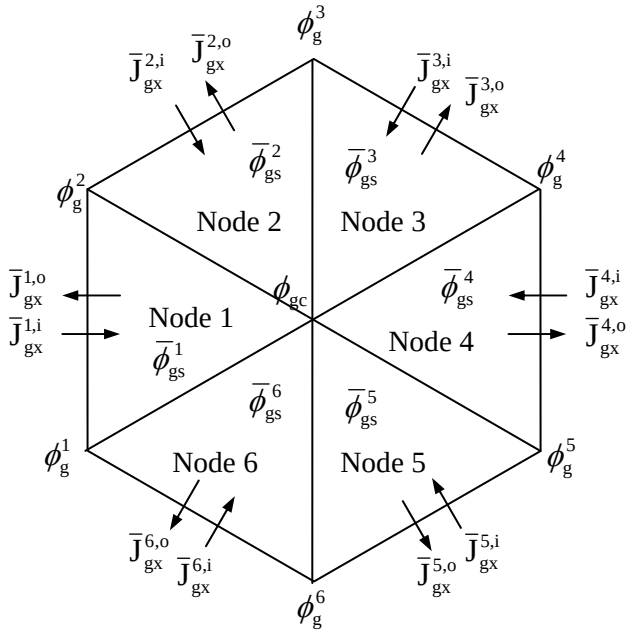

Figure 2-6. Boundary Conditions and Nodal Unknowns on a Hexagonal Node for TPEN

To use the TPEN method, first of all the axial leakage on hexagonal node must be known beforehand. The three-dimensional neutron diffusion equation can be reduced to a two-dimensional one by integrating over the axial direction as:

$$-\mathrm{D}_{\mathrm{g}}^{\mathrm{m}}\left(\frac{\partial^2}{\partial \mathrm{x}^2}+\frac{\partial^2}{\partial \mathrm{y}^2}\right)\phi_{\mathrm{g}}^{\mathrm{m}}(\mathrm{x},\mathrm{y})+\Sigma_{\mathrm{rg}}^{\mathrm{m}}\phi_{\mathrm{g}}^{\mathrm{m}}(\mathrm{x},\mathrm{y}) = \frac{\chi_{\mathrm{g}}}{\mathrm{k}_{\mathrm{eff}}}\sum_{\mathrm{g}'}\nu\Sigma_{\mathrm{fg}'}^{\mathrm{m}}\phi_{\mathrm{g}'}^{\mathrm{m}}(\mathrm{x},\mathrm{y})+\sum_{\mathrm{g}'}\Sigma_{\mathrm{sgg}'}^{\mathrm{m}}\phi_{\mathrm{g}'}^{\mathrm{m}}(\mathrm{x},\mathrm{y})+\mathrm{S}_{\mathrm{gz}}^{\mathrm{m}}(\mathrm{x},\mathrm{y}), \tag{2.2-19}$$

where

$$\phi_{\mathrm{g}}^{\mathrm{m}}(\mathrm{x},\mathrm{y})=\frac{1}{\mathrm{h}_{\mathrm{z}}^{\mathrm{m}}}\int\phi_{\mathrm{g}}^{\mathrm{m}}(\mathrm{x},\mathrm{y},\mathrm{z})\,\mathrm{dz}\,,$$

$$\mathrm{S}_{\mathrm{gz}}^{\mathrm{m}}(\mathrm{x},\mathrm{y})=-\frac{1}{\mathrm{h}_{\mathrm{z}}^{\mathrm{m}}}\int-\mathrm{D}_{\mathrm{g}}^{\mathrm{m}}\frac{\partial^2}{\partial \mathrm{z}^2}\phi_{\mathrm{g}}^{\mathrm{m}}(\mathrm{x},\mathrm{y},\mathrm{z})\,\mathrm{dz} = -\frac{1}{\mathrm{h}_{\mathrm{z}}^{\mathrm{m}}}\left(\mathrm{J}_{\mathrm{gz}}^{\mathrm{m,T}}(\mathrm{x},\mathrm{y})-\mathrm{J}_{\mathrm{gz}}^{\mathrm{m,B}}(\mathrm{x},\mathrm{y})\right).$$

The superscript 'T' and 'B' denote top and bottom surface of node m respectively, and $\mathrm{S}_{\mathrm{gz}}^{\mathrm{m}}$ is the axial leakage source which comes from the axial leakage term. Eq. (2.2-19) means that the radial distribution of the axial leakage source should be pre-determined to obtain a radial solution. In the MASTER code, a NEM solver generates the surface average axial currents that are fed into the TPEN solver as the axial leakage source. The radial shape of the axial leakage source is considered in the following.

Fig.2-7 shows the node average axial leakages for one center and 6 neighboring hexagons. The axial leakage source is defined as:

$$\bar{\mathrm{S}}_{\mathrm{gz}}^{\mathrm{m}}=-\frac{1}{\mathrm{h}_{\mathrm{z}}^{\mathrm{m}}}\left(\bar{\mathrm{J}}_{\mathrm{gz}}^{\mathrm{m,T}}-\bar{\mathrm{J}}_{\mathrm{gz}}^{\mathrm{m,B}}\right). \tag{2.2-20}$$

Using the 7 node average axial leakages shown in Fig. 2-7, the radial dependence of the axial leakage within the central hexagon can be approximated employing a two-dimensional polynomial consisting of 7 independent terms as:

$$S_{gz}(x,y) = d_{g0} + d_{g1}x + d_{g2}y + d_{g3}x^2 + d_{g4}u^2 + d_{g5}p^2 + d_{g6}xup\,. \tag{2.2-21}$$

The 7 coefficients of Eq.(2.2-21) can be determined by imposing 7 node average axial leakage constraints.

The TPEN solver requires three kinds of axial leakage source parameters on a triangle: triangular averaged axial sources, and *x*- and *y*- source moments. Fig. 2-8 shows these axial leakage source parameters of the 6 triangles of the central hexagon which are defined as:

$$\begin{aligned}
\bar{S}_{gz}^{c,n} &= \frac{1}{A^n}\int_{A^n} S_{gz}(x,y)\,dA \quad , \\
\tilde{S}_{gzx}^{c,n} &= \frac{2}{\sqrt{3}h}\frac{1}{A^n}\int_{A^n} xS_{gz}(x,y)\,dA \quad , \\
\tilde{S}_{gzy}^{c,n} &= \frac{2}{h}\frac{1}{A^n}\int_{A^n} yS_{gz}(x,y)\,dA \quad .
\end{aligned} \tag{2.2-22}$$

By inserting Eq.(2.2-21) to (2.2-22), one can obtain axial sources which are expressed by 7 hexagon averaged axial leakage sources of Fig.2-7. For example, the axial sources of the 1st triangle of center hexagon are:

$$\begin{aligned}
\bar{S}_{gz}^{c,1} &= w_1 S_{gz}^c + w_2 S_{gz}^1 + w_3\left(S_{gz}^2 + S_{gz}^6\right) + w_4\left(S_{gz}^3 + S_{gz}^5\right) + w_5 S_{gz}^4, \\
\tilde{S}_{gzx}^{c,1} &= w_{x1} S_{gz}^c + w_{x2} S_{gz}^1 + w_{x3}\left(S_{gz}^2 + S_{gz}^6\right) + w_{x4}\left(S_{gz}^3 + S_{gz}^5\right) + w_{x5} S_{gz}^4, \\
\tilde{S}_{gzy}^{c,1} &= w_{y1}\left(S_{gz}^2 - S_{gz}^6\right) + w_{y2}\left(S_{gz}^3 - S_{gz}^5\right).
\end{aligned} \tag{2.2-23}$$

where

$$w_1 = 1, \quad w_2 = \frac{83}{540}, \quad w_3 = \frac{17}{540}, \quad w_4 = -\frac{37}{540}, \quad w_5 = -\frac{43}{540},$$

$$w_{x1} = -\frac{1}{54}, \quad w_{x2} = \frac{59}{3240}, \quad w_{x3} = \frac{7}{1620}, \quad w_{x4} = -\frac{1}{324}, \quad w_{x5} = -\frac{7}{3240},$$

$$w_{y1} = -\frac{1}{40}, \quad w_{y2} = -\frac{1}{360}.$$

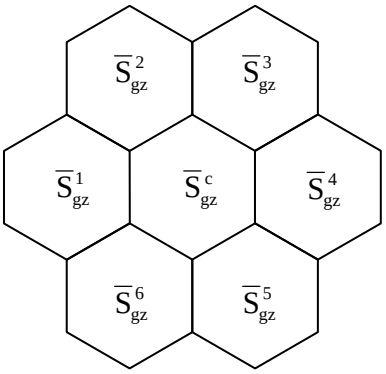

Figure 2-7. Notations for Axial Sources near Center Hexagon

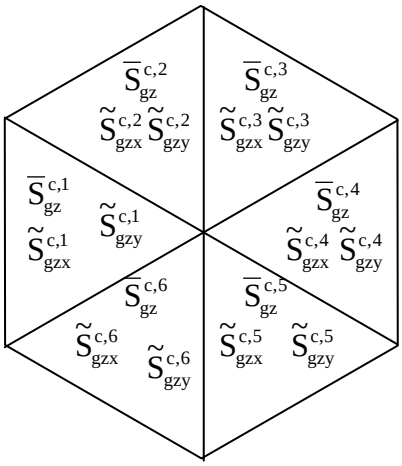

Figure 2-8. Triangular Axial Leakage Source Parameters